

Strange-Particle Production in π^-p Interactions from 1.5 to 4.2 BeV/c. II. Two-Body Final States*

ORIN I. DAHL, LYNDON M. HARDY,† RICHARD I. HESS,‡ JANOS KIRZ, DONALD H. MILLER,
AND JOSEPH A. SCHWARTZ§

Department of Physics and Lawrence Radiation Laboratory, University of California, Berkeley, California

(Received 6 March 1967)

The reactions $\pi^-p \rightarrow \Lambda K^0$, $\Sigma^0 K^0$, and $\Sigma^- K^+$ in the 1.5- to 4.2-BeV/c momentum range were studied in the Lawrence Radiation Laboratory's 72-in. hydrogen bubble chamber. The total cross sections for the three reactions decrease as $E_{c.m.}^{-3.6}$, $E_{c.m.}^{-3.3}$, and $E_{c.m.}^{-2.3}$, respectively. The differential cross sections are presented at 11 beam momenta. A peripheral peak is the dominant feature of the reactions $\pi^-p \rightarrow \Lambda K^0$ and $\Sigma^0 K^0$, for which K^* exchange is allowed, but no such peaking is seen in $\pi^-p \rightarrow \Sigma^- K^+$. An exponential fit to the momentum-transfer distributions in the peripheral region yields slope parameters in the 6- to 10-(BeV/c)⁻² range. The differential cross sections for $\pi^-p \rightarrow \Lambda K^0$ and $\Sigma^- K^+$ show peaking for forward production of hyperons in the c.m. system, to which baryon exchange is expected to contribute. The angular distribution of the Λ polarization in $\pi^-p \rightarrow \Lambda K^0$ is presented.

I. INTRODUCTION

NUMEROUS authors have reported results on the associated production reactions

$$\pi^-p \rightarrow \Lambda K^0 \quad (1)$$

$$\Sigma^0 K^0 \quad (2)$$

$$\Sigma^- K^+ \quad (3)$$

at energies from threshold to 1.5 BeV/c.¹ This work is

* This work was done under the auspices of the U. S. Atomic Energy Commission. Part of this paper is from a thesis submitted by J. A. Schwartz to the Graduate Division of the University of California, Berkeley, California in partial fulfillment of the requirements for the degree of Doctor of Philosophy.

† Present address: TRW Systems, Inc., 1 Space Park, Redondo Beach, California.

‡ Present address: Logicon, Inc., 205 Avenue I, Redondo Beach, California.

§ Present address: College of Physicians and Surgeons, Columbia University, 722 W. 168th Street, New York, New York.

¹ Some of the reports on strange-particle production up to 1.5 BeV/c are: L. Bertanza, P. L. Connolly, B. B. Culwick, F. R. Eisler, T. Morris, R. Palmer, A. Prodell, and N. P. Samios, *Phys. Rev. Letters* **8**, 332 (1962) (900, 920, 960, and 1000 MeV/c); F. S. Crawford, Jr., M. Cresti, R. L. Douglass, M. L. Good, G. R. Kalbfleisch, M. L. Stevenson, and H. K. Ticho, in *Ninth Annual International Conference on High-Energy Physics, Kiev, 1959* [Academy of Science (IUPAP), Moscow, 1960], Vol. 1, p. 443 (940 to 1220 MeV/c); Joseph Keren, *Phys. Rev.* **133**, B457 (1964) (1020 MeV/c); J. A. Anderson, F. S. Crawford, B. B. Crawford, R. L. Golden, L. J. Lloyd, G. W. Meisner, and L. R. Price, in *Proceedings of the 1962 Annual International Conference on High-Energy Physics at CERN* (CERN, Geneva, 1962), p. 270 (1035, 1220 MeV/c); F. Eisler, R. Plano, A. Prodell, N. Samios, M. Schwartz, J. Steinberger, P. Bassi, V. Borelli, G. Puppi, G. Tanaka, P. Waloschek, V. Zoboli, M. Conversi, P. Franzini, I. Mannelli, R. Santangelo, V. Silverstrini, D. A. Glaser, C. Graves, and M. L. Perl, *Phys. Rev.* **108**, 1353 (1957) (1040, 1080, and 1230 MeV/c); *Nuovo Cimento* **10**, 468 (1958) (1040, 1090, 1330, 1430 MeV/c); L. B. Leipuner and R. K. Adair, *Phys. Rev.* **109**, 1358 (1958) (1090 MeV/c); Y. S. Kim, G. R. Burleson, P. I. P. Kalmus, A. Roberts, C. L. Sandler, and T. A. Romanowski, *ibid.* **151**, 1090 (1966) (1.17, 1.32 BeV/c); F. S. Crawford, Jr., M. Cresti, M. L. Good, K. Gottstein, E. M. Lyman, F. T. Solmitz, M. L. Stevenson, and H. K. Ticho, in *Proceedings of the 1958 Annual International Conference on High-Energy Physics at CERN* (CERN, Geneva, 1958), p. 323 (1120 MeV/c); J. A. Anderson, Lawrence Radiation Laboratory Report No. UCRL-10838, 1963 (unpublished) (1170 MeV/c); F. S. Crawford, Jr., R. L. Douglas, M. L. Good, G. R. Kalbfleisch, M. L. Stevenson, and H. K.

an extension of these studies into the energy range 1.5 to 4.2 BeV/c. Recently experiments have also been performed in this momentum range²⁻⁷ and at higher energies.⁸⁻¹¹

This experiment was performed at the Bevatron with the 72-in. bubble chamber. The experimental procedure, and results on three- and more-body final states are reported in the preceding paper.¹² We refer the reader to that paper for details on the analysis of the data. Here we discuss only those features relevant to the two-body final states ΛK^0 , $\Sigma^0 K^0$, and $\Sigma^- K^+$.

Our sample, based on 890 000 pictures, consists of 4300 ΛK^0 events, 1200 $\Sigma^0 K^0$ events, and 2600 $\Sigma^- K^+$ events. This sample satisfies the following selection criteria: For the ΛK^0 final state we use events for which either $\Lambda \rightarrow p\pi^-$ or $K^0 \rightarrow \pi^+\pi^-$ or both decays are observed within the fiducial volume. For the $\Sigma^0 K^0$ final state we require that $K^0 \rightarrow \pi^+\pi^-$ be observed. For the

Ticho, *Phys. Rev. Letters* **3**, 394 (1959) (1220 MeV/c); J. L. Brown, D. A. Glaser, D. I. Meyer, M. L. Perl, J. Vander Velde, and J. W. Cronin, *Phys. Rev.* **107**, 906 (1957) and J. L. Brown, D. A. Glaser, and M. L. Perl, *ibid.* **108**, 1036 (1957) (1230 MeV/c).

² L. L. Yoder, C. T. Coffin, D. I. Meyer, and K. M. Terwilliger, *Phys. Rev.* **132**, 1778 (1963) (1508 MeV/c).

³ O. Goussu, M. Sené, B. Ghidini, S. Mongelli, A. Romano, P. Waloschek, and V. Alles-Borelli, *Nuovo Cimento* **42**, A606 (1966) (1.59 BeV/c).

⁴ D. H. Miller, A. Z. Kovacs, R. McIlwain, T. R. Palfrey, and G. W. Tautfest, *Phys. Rev.* **140**, B360 (1965) (2.7 BeV/c).

⁵ O. Goussu, G. Smadja, and G. Kayas, *Nuovo Cimento* **47**, A383 (1967) (2.75 BeV/c).

⁶ T. P. Wangler, A. R. Erwin, and W. D. Walker, *Phys. Rev.* **137**, B414 (1965) (3.0 BeV/c).

⁷ Aachen-Hamburg-London-München Collaboration, *Nuovo Cimento* **43**, A1010 (1966) (4.0 BeV/c).

⁸ L. Bertanza, B. B. Culwick, K. W. Lai, I. S. Mitra, N. P. Samios, A. M. Thorndike, S. S. Yamamoto, and R. M. Lea, *Phys. Rev.* **130**, 786 (1963) (4.65 BeV/c).

⁹ D. J. Crennell, G. R. Kalbfleisch, K. W. Lai, J. M. Scarr, T. G. Schumann, I. O. Skillicorn, and M. S. Webster, *Phys. Rev. Letters* **18**, 86 (1967) (6 BeV/c).

¹⁰ R. Ehrlich, W. Selove, and H. Yuta, *Phys. Rev.* **152**, 1194 (1966) (7.91 BeV/c).

¹¹ A. Bigi, S. Brandt, A. deMarco-Trabucco, Ch. Peyrou, R. Sosnowski, and A. Wroblewski, *Nuovo Cimento* **33**, 1249 (1964) (10 BeV/c).

¹² O. I. Dahl, L. M. Hardy, R. I. Hess, J. Kirz, and D. H. Miller, preceding paper, *Phys. Rev.* **163**, 1377 (1967).

TABLE I. Cross section for associated production.

p_{beam}^a (BeV/c)	$E_{\text{c.m.}}$ (BeV)	$\pi^-p \rightarrow \Lambda K^0$		$\pi^-p \rightarrow \Sigma^0 K^0$		$\pi^-p \rightarrow \Sigma^- K^+$		Reference	Symbol on Fig. 1
		σ (μb)	Events	σ (μb)	Events	σ (μb)	Events		
1.50	1.930	334±19	308	167±22	59	242 +14	293	14	▽
1.508	1.934	214±23	476	~177	134			2	◇
1.59	1.974	214±21	106 ^b	178±22	65	262 ±16	285	3	▲
1.615	1.985	208±25	286	111±20	70	180 ±20	319	Present expt.	○
1.69	2.020	199±12	263	110±14	58	153 ± 9	266	14	▽
1.85	2.093	181±12	215	140±17	66	99 ± 8	153	14	▽
1.94	2.133	185±15	436	126±15	127	98 ±10	281	Present expt.	○
1.95	2.137	182±11	255	94±13	53	99 ± 7	182	14	▽
1.98	2.150	184±20	299	116±15	87	90 ±10	191	Present expt.	○
2.05	2.181	182±17	119	123±21	33	70 ± 9	60	14	▽
2.05	2.181	179±15	515	113±10	153	87 ± 8	327	Present expt.	○
2.14	2.219	162±20	78	100±20	23	39 ±10	25	Present expt.	○
2.15	2.223	192±11	334	114±13	82	65 ± 5	148	14	▽
2.25	2.265	172±10	319	105±12	80	57 ± 5	138	14	▽
2.35	2.310	174±14	157	113±18	41	53 ± 7	63	14	▽
2.605	2.407	106±12	182	81±12	66	30 ± 5	67	Present expt.	○
2.70	2.444	120±11		85±12		31 ± 5		4	■
2.75	2.463	90±25	18	95±25	19	32 ±10	15	5	◆
2.86	2.505	109±15	59	93±25	26	22 ± 7	18	Present expt.	○
3.00	2.556	31±14	5	86±25	14	15 ± 5	12	6	●
3.01	2.560	84±12	111	74±12	52	22 ± 4	43	Present expt.	○
3.125	2.602	94±12	170	41±10	39	15.5± 3.0	41	Present expt.	○
3.21	2.632	87±10	301	50± 6	91	15.5± 2.0	76	Present expt.	○
3.885	2.862	67±12	86	37± 8	22	8.5± 2.5	16	Present expt.	○
4.00	2.900	c		c		5.0± 3.0	2	7	△
4.16	2.948	49± 8	75	42± 8	30	4.5± 1.5	10	Present expt.	○
4.65	3.103	d		d			0	8	○

^a The momentum bite is typically between ± 0.03 and ± 0.05 BeV/c.

^b This value does not include events where only a $\Lambda \rightarrow p\pi^-$ decay is seen.

^c $\sigma(\pi^-p \rightarrow \Lambda K^0) + \sigma(\pi^-p \rightarrow \Sigma^0 K^0) = 93 \pm 14 \mu\text{b}$ based on 39 events is given in Ref. 7.

^d $\sigma(\pi^-p \rightarrow \Lambda K^0) + \sigma(\pi^-p \rightarrow \Sigma^0 K^0) = 40 \mu\text{b}$ based on 8 events is reported in Ref. 8.

$\Sigma^- K^+$ final state we require the $\Sigma^- \rightarrow n\pi^-$ decay be

bility that the above requirements are met.

Once the consistency of the kinematic fits with bubble density is verified on the scan table, reaction (3) is well enough constrained that the sample is essentially uncontaminated. The same holds true for reactions (1) and (2) if both the Λ and K^0 decays are observed. If only one decay is observed, assignment of events is based on missing-mass selection criteria.¹³ By reprocessing the well-constrained two-decay events as if only one decay were observed, we found that the cross contamination between the Λ and Σ^0 channels for the whole sample is less than 10% at all beam momenta.

II. TOTAL CROSS SECTIONS

For cross-section measurements only, the experiment was divided into two parts. Results on the first part ($\pi 72$) have been given by Schwartz,¹⁴ and are merely quoted here. In this case, the total number of interactions was estimated from a scan of every fifth frame

¹³ If only a $K^0 \rightarrow \pi^+\pi^-$ decay is seen, the event is admitted to the sample if the square of the missing mass is $1.15 (\text{BeV})^2 < \text{MM}^2 < 1.56 (\text{BeV})^2$. If only a $\Lambda \rightarrow p\pi^-$ decay is seen, the limits are $0.2 (\text{BeV})^2 < \text{MM}^2 < 0.3 (\text{BeV})^2$. Cross-section values are corrected for the loss of events due to these cuts.

¹⁴ Joseph A. Schwartz, Lawrence Radiation Laboratory Report No. UCRL-11360, 1964 (unpublished).

in a randomly chosen sample of film; frames with more than 22 tracks (TMT's) were treated separately. A sample of 270 TMT's was scanned, yielding a mean of 28.3 tracks/TMT; the total number of interactions at each beam momentum was prorated accordingly. Corrections of $+2 \pm 2\%$ for scanning efficiency, and -2.5% for events falling outside the fiducial volume were applied; the path length corresponding to the total number of interactions at each momentum was calculated using the cross-section values reported by Diddens *et al.*¹⁵

In the second part ($\pi 63$) a selected sample of film was scanned completely for all interactions in each momentum interval. The number of observed two-prong events was corrected by $+10 \pm 3\%$ to account for unnoticed small-angle scatterings. Using the information from this special scan, and with the data of Diddens *et al.*¹⁵ and Citron *et al.*,¹⁶ we determined the cross section per event found in the general scan. Final cross sections were determined by comparing the corrected number of fitted events of a given type with the corresponding number of events found in the general scan. This procedure is described in detail in the preceding paper.¹²

Since cross-section determinations were not identical,

¹⁵ A. N. Diddens, E. W. Jenkins, T. F. Kycia, and K. F. Riley, Phys. Rev. Letters **10**, 262 (1963).

¹⁶ A. Citron, W. Galbraith, T. F. Kycia, B. A. Leontic, R. H. Phillips, and A. Rousset, Phys. Rev. Letters **13**, 205 (1964); Phys. Rev. **144**, 1101 (1966).

there may be small systematic differences in the two parts of the experiment. Our results, as well as those of other experiments²⁻⁸ are presented in Table I. In Fig. 1 the same data are plotted on a log-log scale as a function of total c.m. energy, $E_{c.m.}$. In each case the cross section decreases monotonically with increasing energy. Since the data in Fig. 1 lie essentially on three straight lines, they have been fitted with

$$\sigma_T = A E_{c.m.}^B. \quad (4)$$

This expression provides adequate fits to reactions (2) and (3). For the $\Sigma^0 K^0$ final state, the least-squares fit gives $B = -3.30 \pm 0.30$, with $\chi^2 = 24.6$ for 24 data points. For the $\Sigma^- K^+$ final state, we have $B = -9.30 \pm 0.25$ with $\chi^2 = 34.5$ for 25 data points. For the ΔK^0 final state, we have $B = -3.57 \pm 0.20$ with $\chi^2 = 60.1$ for 25 data points; consequently, in this case the fit is poor.

We have considered the possibility that the poor fit in the ΔK^0 channel reflects a significant contribution to the cross section from s -channel resonances. It is not difficult to see that a better fit to $\sigma_T(\Delta K^0)$ in Fig. 1 may be obtained with a linear "background" and a peak superimposed near $E_{c.m.} \approx 2200$ MeV. It appears reasonable to identify this with $N_{1/2}^*(2190)$; however, most data with $E_{c.m.} < 2350$ MeV represent ($\pi 72$),

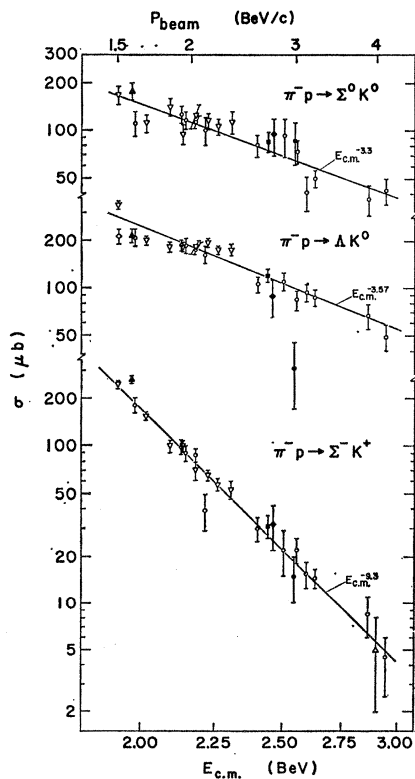


FIG. 1. Total cross sections as a function of the total c.m. energy for the reactions $\pi^- p \rightarrow \Delta K^0$, $\pi^- p \rightarrow \Sigma^0 K^0$, and $\pi^- p \rightarrow \Sigma^- K^+$. Log-log scale is used. The lines represent least-squares fits of the data to the expression $\sigma_T = A E_{c.m.}^B$. The symbols are explained in Table I.

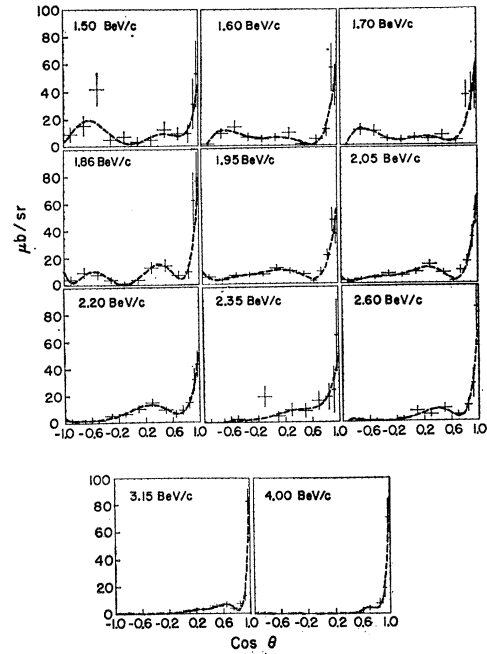


FIG. 2. Differential cross sections for the reaction $\pi^- p \rightarrow \Delta K^0$. The angle θ is defined by $\cos \theta = \hat{P}_{K^0} \cdot \hat{P}_{beam}$ in the reaction c.m. system. The curves correspond to least-squares fits of Legendre polynomials to the data. The data are also given in Table II, and the values for the parameters of the fits in Table III.

while most data with $E_{c.m.} > 2350$ MeV were obtained in ($\pi 63$). Consequently, possible systematic differences in normalization are crucial. Should the peak represent a contribution from decay of $N_{1/2}^*(2190)$, characteristic structure will appear in angular distributions and polarizations, these considerations are discussed further in Secs. III and IV.

Recently, Morrison pointed out the existence of strong regularities in the energy dependences of cross sections for a large number of reactions.¹⁷ By fitting measured cross sections to the expression

$$\sigma_T = C (p_{in}/p_0)^{-n}, \quad (5)$$

where p_{in} is the beam momentum in the laboratory system and p_0 is a constant, he found that values of the exponent n fall into at least three distinct groups. When the reaction can be interpreted as exchange of a nonstrange meson, $n \approx 1.5$; when the reaction involves exchange of a strange meson, $n \approx 2.0$; when the reaction occurs through baryon exchange, $n \approx 4.0$.

For comparison, the data in the present experiment have been fitted to expression (5). We find that $n = 1.45 \pm 0.08$ for $\pi^- p \rightarrow \Delta K^0$; $n = 1.36 \pm 0.13$ for $\pi^- p \rightarrow \Sigma^0 K^0$; and $n = 3.78 \pm 0.10$ for $\pi^- p \rightarrow \Sigma^- K^+$. Since the isotopic spin is $\frac{1}{2}$ for all presently known strange mesons, it is likely that only the ΔK^0 and $\Sigma^0 K^0$ final states can be

¹⁷ D. R. O. Morrison, review paper delivered at the Conference on Two-Body Reactions, Stony Brook, April 1966 (to be published).

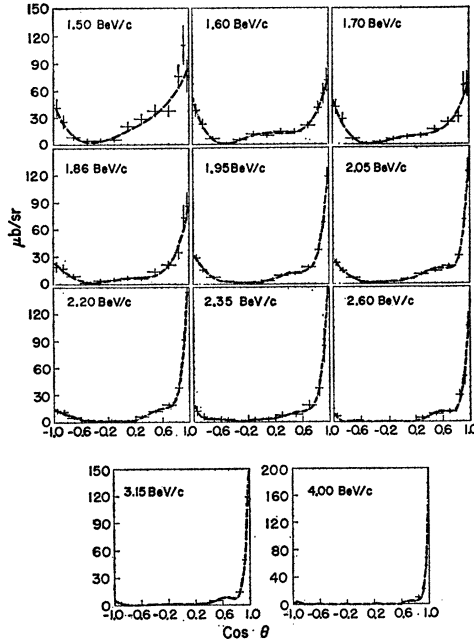


FIG. 3. Differential cross sections for the reaction $\pi^-p \rightarrow \Sigma^0 K^0$. The angle θ is defined by $\cos\theta = \hat{p}_{K^0} \cdot \hat{p}_{\text{beam}}$ in the reaction c.m. system. The curves correspond to least-squares fits of Legendre polynomials to the data. The data are also given in Table II, and the values for the parameters of the fits in Table III.

produced through single-meson exchange. For the $\Sigma^- K^+$ final state, the simplest production mechanism involves baryon exchange. Consequently the observed

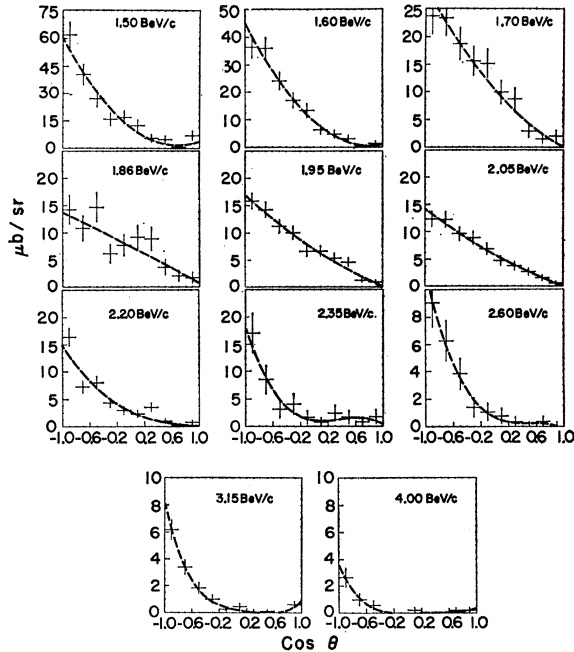


FIG. 4. Differential cross sections for the reaction $\pi^-p \rightarrow \Sigma^- K^+$. The angle θ is defined by $\cos\theta = \hat{p}_{K^+} \cdot \hat{p}_{\text{beam}}$ in the reaction c.m. system. The curves correspond to least-squares fits of Legendre polynomials to the data. The data are also given in Table II, and the values for the parameters of the fits in Table III.

n values are roughly consistent with the pattern suggested by Morrison; however, over the energy range studied they do not support the distinction between reactions involving exchange of strange and nonstrange mesons.

III. DIFFERENTIAL CROSS SECTIONS

For the analysis of differential cross sections the data were divided into 11 momentum bins centered at $p_{\text{in}} = 1.50, 1.60, 1.70, 1.86, 1.95, 2.05, 2.20, 2.35, 2.60, 3.15,$

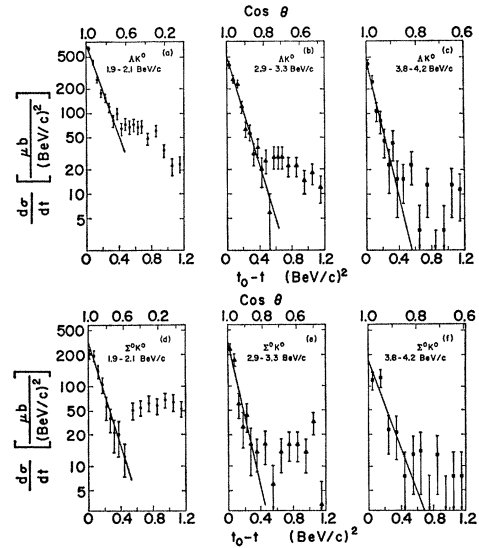


FIG. 5. Momentum-transfer distribution in the region of peripheral peaking (a)–(c) for $\pi^-p \rightarrow \Lambda K^0$ and (d)–(f) for $\pi^-p \rightarrow \Sigma^0 K^0$. The lines represent maximum-likelihood fits to the expression $d\sigma/dt = C \exp[-D(t_0 - t)]$ in the region $0 < t_0 - t < 0.4$ (BeV/c)². The beam momenta and the fitted slope parameters are as follows. For $\pi^-p \rightarrow \Lambda K^0$:

- (a) 1.9–2.1 BeV/c , $D = 6.4 \pm 0.5$ (BeV/c)⁻²;
- (b) 2.9–3.3 BeV/c , $D = 7.7 \pm 0.6$ (BeV/c)⁻²;
- (c) 3.8–4.2 BeV/c , $D = 9.9 \pm 1.1$ (BeV/c)⁻².

For $\pi^-p \rightarrow \Sigma^0 K^0$:

- (d) 1.9–2.1 BeV/c , $D = 7.5 \pm 1.0$ (BeV/c)⁻²;
- (e) 2.9–3.3 BeV/c , $D = 10.7 \pm 1.2$ (BeV/c)⁻²;
- (f) 3.8–4.2 BeV/c , $D = 6.3 \pm 2.0$ (BeV/c)⁻².

and 4.0 BeV/c . For the first nine bins, Δp_{in} is ± 50 MeV/c ; for the bins centered at $p_{\text{in}} = 3.15$ and 4.0 BeV/c , events were accepted with $2.9 \leq p_{\text{in}} \leq 3.3$ BeV/c and $3.8 \leq p_{\text{in}} \leq 4.2$ BeV/c , respectively.

The results are summarized in Table II, and are plotted in Figs. 2 to 4. The dashed curves represent least-squares fits to

$$\frac{d\sigma}{d\Omega} = \sum_n A_n P_n(\cos\theta), \quad (6)$$

where P_n are Legendre polynomials, and θ is the c.m.

TABLE II. Differential cross section in units of $\mu\text{b}/\text{sr}$ as a function of the beam momentum and the production angle.

$\frac{p_{\text{beam}}}{(\text{BeV}/c)} \setminus \cos\theta$	$\pi^- p \rightarrow \Lambda K^0$												
	-1.0	-0.9	-0.8	-0.6	-0.4	-0.2	0.0	0.2	0.4	0.6	0.8	0.95	1.0
1.50	41.6±9.6	25.8±7.2	8.6±2.9	4.7±2.1	4.6±2.1	5.5±2.3	20.6±4.4	28.8±5.2	37.9±6.0	37.7±6.0	76.0±12.2	110.2±20.8	76.6±17.6
1.60	38.5±6.6	23.0±5.1	6.5±1.8	1.1±0.8	5.0±1.6	11.3±2.4	9.9±2.2	14.2±2.7	13.8±2.6	20.9±3.2	40.8±6.5	56.4±10.9	71.3±12.4
1.70	41.9±7.8	28.4±6.2	6.5±2.0	1.3±0.9	2.5±1.3	5.8±1.9	8.2±2.3	9.5±2.5	16.5±3.2	24.7±4.0	30.4±6.3	65.5±13.4	66.8±13.6
1.86	19.2±5.0	17.1±4.6	8.9±2.3	1.8±1.0	4.1±1.5	4.7±1.7	6.9±2.0	6.3±1.9	13.8±2.8	21.3±3.6	34.8±6.5	73.7±13.5	86.5±14.8
1.95	29.0±3.2	15.9±2.3	7.8±1.1	3.0±0.7	1.7±0.5	2.1±0.6	3.8±0.8	9.4±1.2	11.8±1.4	18.6±1.7	37.5±3.5	68.2±6.8	118.4±9.1
2.05	23.1±3.2	14.4±2.5	6.8±1.2	1.9±0.6	2.1±0.7	2.5±0.7	5.2±1.0	10.4±1.5	14.0±1.7	19.0±2.0	30.4±3.6	70.3±7.9	122.9±10.6
2.20	12.8±2.5	11.3±2.3	5.2±1.1	2.5±0.8	1.3±0.5	2.1±0.7	1.7±0.6	6.1±1.2	11.9±1.6	19.1±2.0	38.1±4.1	91.6±9.1	144.6±11.7
2.35	12.4±5.1	5.9±3.4	3.1±1.8	2.9±1.7	1.0±1.0	2.9±1.7	3.2±1.9	7.7±2.7	8.6±2.9	18.6±4.3	37.4±8.6	84.6±18.5	168.5±26.6
2.60	6.7±2.5	0.0±0.9	1.4±0.8	0.0±0.5	0.9±0.7	0.9±0.6	0.0±0.5	4.4±1.4	8.7±2.0	11.2±2.2	29.5±5.2	50.5±9.7	106.4±14.5
3.15	3.5±0.9	1.2±0.5	0.0±0.1	0.3±0.2	0.8±0.3	1.3±0.4	0.9±0.3	2.1±0.5	5.0±0.8	8.1±1.0	14.3±1.8	49.7±4.9	119.0±7.8
4.00	3.1±1.4	1.2±0.9	0.3±0.3	0.0±0.3	0.0±0.3	0.0±0.3	0.0±0.3	0.4±0.4	0.0±0.6	3.6±1.1	10.1±2.5	22.7±5.2	123.0±12.3

$\frac{p_{\text{beam}}}{(\text{BeV}/c)} \setminus \cos\theta$	$\pi^- p \rightarrow \Sigma^0 K^0$												
	-1.0	-0.8	-0.6	-0.4	-0.2	0.0	0.2	0.4	0.6	0.8	0.95	1.0	
1.50	9.1±5.2	15.5±7.1	42.1±11.5	4.8±3.4	6.9±4.0	3.3±3.3	4.5±3.2	12.2±5.5	9.0±4.5	9.1±6.5	30.9±18.1	52.8±23.9	
1.60	1.5±1.5	9.2±3.5	14.0±4.2	6.2±2.8	4.8±2.4	5.9±2.7	9.4±3.3	7.2±1.2	4.8±2.4	12.0±5.4	57.0±17.4	44.2±14.7	
1.70	0.0±1.1	11.1±4.0	10.1±3.9	4.6±2.3	3.9±2.3	5.5±2.5	4.4±2.2	7.2±3.0	3.3±1.9	36.4±9.5	38.1±13.5	40.1±14.3	
1.86	3.9±2.8	9.1±3.8	7.6±3.1	3.7±2.1	1.2±1.2	3.7±2.1	12.8±4.1	14.4±4.4	7.2±2.9	9.7±4.9	62.9±20.1	77.1±20.8	
1.95	5.5±1.7	3.2±1.1	6.5±1.6	6.7±1.6	7.2±1.7	11.5±2.2	9.3±1.9	7.1±1.7	5.5±1.5	21.0±4.0	47.1±8.5	36.8±7.5	
2.05	2.3±1.1	3.3±1.2	4.2±1.4	7.0±1.8	5.8±1.6	8.3±1.9	13.6±2.5	7.7±1.8	5.5±1.5	16.0±3.8	34.0±7.8	53.1±9.9	
2.20	2.0±1.2	1.7±1.0	1.9±0.9	5.0±1.6	6.3±1.8	10.1±2.4	14.7±2.7	9.3±2.2	7.6±2.0	14.6±4.0	31.6±8.0	43.0±9.5	
2.35	0.0±2.4	0.0±2.4	2.4±2.4	0.0±2.4	19.0±7.4	4.6±3.2	9.0±4.5	8.4±5.0	15.8±6.6	18.7±9.4	23.7±16.8	63.8±26.4	
2.60	0.0±1.0	1.0±1.0	1.0±1.0	0.0±1.0	2.0±1.4	7.7±2.7	5.0±2.2	9.4±3.0	4.7±2.1	11.4±4.7	27.6±10.4	84.2±18.4	
3.15	0.3±0.3	0.3±0.3	0.0±0.3	0.3±0.3	0.7±0.4	2.0±0.7	3.2±0.9	5.6±1.2	5.4±1.2	7.4±1.9	13.2±3.6	82.0±9.3	
4.00	0.0±0.6	0.0±0.6	0.0±0.6	0.0±0.6	0.0±0.6	0.0±0.6	0.0±0.6	0.6±0.6	4.2±1.6	7.7±3.2	19.0±6.7	70.5±13.7	

$\frac{p_{\text{beam}}}{(\text{BeV}/c)} \setminus \cos\theta$	$\pi^- p \rightarrow \Sigma^- K^+$												
	-1.0	-0.8	-0.6	-0.4	-0.2	0.0	0.2	0.4	0.6	0.8	0.95	1.0	
1.50	62.0±6.8	40.5±5.6	27.1±4.5	16.0±3.5	17.0±2.7	16.9±3.6	12.4±3.1	5.5±2.1	4.8±2.0	4.8±2.0	0.8±0.8	7.0±2.5	
1.60	36.5±3.9	36.0±3.8	24.1±3.2	17.0±2.7	13.4±2.4	13.4±2.4	6.3±1.6	4.8±1.4	3.1±1.2	3.1±1.2	0.4±0.4	1.4±0.8	
1.70	23.7±3.2	23.4±3.2	18.7±2.9	15.6±2.6	15.2±2.7	15.2±2.7	9.9±2.1	8.7±2.0	2.9±1.2	2.9±1.2	1.5±0.9	2.0±1.0	
1.86	14.3±2.6	10.8±2.3	14.7±2.6	6.2±1.7	7.7±1.9	7.7±1.9	9.2±2.1	8.9±2.1	3.7±1.4	3.7±1.4	2.1±1.0	1.7±1.0	
1.95	15.8±1.4	14.3±1.3	11.2±1.2	10.0±1.1	6.6±0.9	6.6±0.9	6.7±0.9	5.3±0.8	4.6±0.8	4.6±0.8	1.2±0.4	0.9±0.4	
2.05	12.3±1.4	12.2±1.4	9.7±1.2	8.9±1.2	8.9±1.2	6.9±1.1	4.7±0.9	3.8±0.8	2.7±0.7	2.7±0.7	1.5±0.5	0.6±0.3	
2.20	16.4±1.6	7.2±1.1	7.9±1.1	4.4±0.8	3.0±0.7	3.0±0.7	2.3±0.6	3.5±0.8	1.0±0.4	1.0±0.4	0.8±0.4	0.8±0.4	
2.35	17.0±3.6	8.5±2.6	3.1±1.6	4.0±1.8	1.6±1.2	1.6±1.2	2.4±1.4	2.4±1.4	1.7±1.2	1.7±1.2	0.8±0.8	1.8±1.2	
2.60	9.1±1.8	6.3±1.5	3.8±1.2	1.4±0.7	1.1±0.6	1.1±0.6	0.8±0.6	0.4±0.4	0.0±0.1	0.0±0.1	0.4±0.4	0.0±0.4	
3.15	6.2±0.7	3.4±0.5	1.8±0.4	1.0±0.3	0.3±0.2	0.3±0.2	0.3±0.2	0.0±0.1	0.0±0.1	0.0±0.1	0.0±0.1	0.6±0.3	
4.00	2.6±0.7	1.0±0.4	0.6±0.3	0.0±0.2	0.0±0.2	0.0±0.2	0.2±0.2	0.0±0.2	0.0±0.2	0.0±0.2	0.2±0.2	0.2±0.2	

production angle¹⁸; the fitted coefficients A_n are given in Table III.

The dominant characteristics of the angular distributions are: (a) sharp peaking near $\cos\theta = +1$ for both the ΔK^0 and $\Sigma^0 K^0$ channels which may be mediated by single-meson exchange; (b) peaking near $\cos\theta = -1$ for the $\Sigma^- K^+$ channel which can occur only through baryon exchange; and (c) the smaller peak near $\cos\theta = -1$ for the ΔK^0 channel. We discuss each of these features in turn.

Rather than use $\cos\theta$, it is convenient to introduce the square of the four-momentum transfer

$$t = (E_Y - E_p)^2 - (\mathbf{p}_Y - \mathbf{p}_p)^2, \quad (7)$$

which is Lorentz invariant. The subscripts Y and p denote the hyperon and proton, respectively. In the c.m.

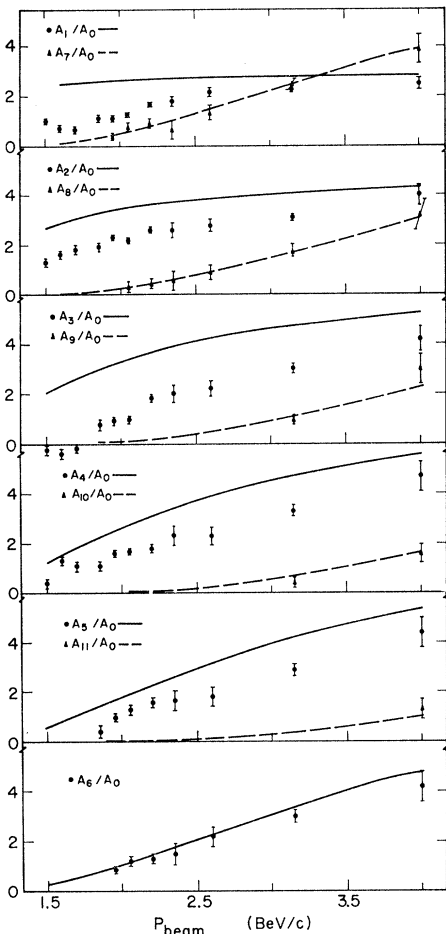


FIG. 6. Coefficients of the Legendre-polynomial fit to the $\pi^- p \rightarrow \Lambda K^0$ angular distribution as a function of the beam momentum. The curves represent the expansion of the function $d\sigma/dt = C \exp[-7(t_0 - t)]$ in terms of Legendre polynomials.

¹⁸ The following guideline was used for selecting the highest-order polynomial used for fitting the angular distributions: Once the need for a certain order is indicated by a rise of the confidence level in the fit, at least that order is used for all higher beam momenta.

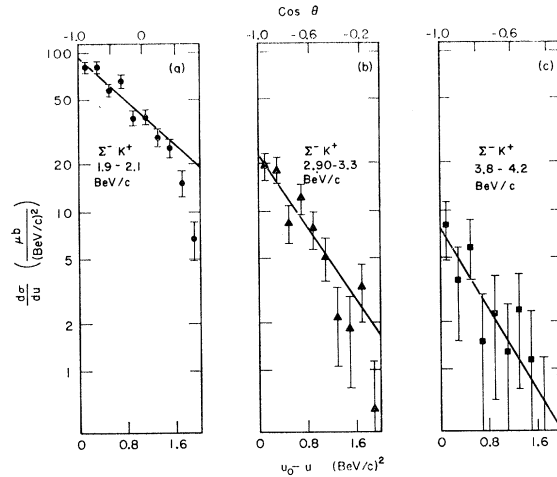


FIG. 7. Momentum-transfer distribution in the u channel for $\pi^- p \rightarrow \Sigma^- K^+$. The lines represent maximum-likelihood fits to the expression $d\sigma/du = C \exp[-D(u_0 - u)]$ in the region $0 < u_0 - u < 1$ (BeV/c)². The beam momenta and the fitted slope parameters are (a) 1.9–2.1 BeV/c , $D = 0.79 \pm 0.12$ (BeV/c)⁻²; (b) 2.9–3.3 BeV/c , $D = 1.30 \pm 0.30$ (BeV/c)⁻²; (c) 3.8–4.2 BeV/c , $D = 1.45 \pm 0.8$ (BeV/c)⁻².

system $dt = 2p_Y p_p d(\cos\theta)$. The maximum value t_0 occurs at $\cos\theta = +1$. The distributions in $t_0 - t$ are shown in Fig. 5 for the ΔK^0 and $\Sigma^0 K^0$ final states. The lines represent maximum-likelihood fits to the expression

$$\frac{d\sigma}{dt} = C \exp[-D(t_0 - t)] \quad (8)$$

over the region $0 \leq t_0 - t \leq 0.4$ (BeV/c)². Over the energy range covered in this experiment, secondary maxima in the differential cross sections are significant. When a wider interval of momentum transfer is included in the fit, the slope D changes beyond the range of errors. Consequently, the fit shown in Fig. 5 must be considered qualitative.¹⁹

To explore further the connection between the Legendre and the exponential fits, expression (8) was expanded in Legendre polynomials.²⁰ For this calculation we set D equal to 7 (BeV/c)⁻²; to avoid problems of normalization, the ratios A_n/A_0 for each beam momentum were compared with the corresponding fitted quantities from Table III. On Fig. 6 this comparison is shown for the ΔK^0 final state. Clearly, for the low-order

¹⁹ The break in the roughly exponential distribution near $t = -0.5$ (BeV/c)² and the secondary peak at larger values of $|t|$ in the $\Sigma^0 K^0$ channel is a common feature of many two-body reactions. The dip near $t = -0.5$ (BeV/c)² in the reaction $\pi^- p \rightarrow \pi^0 n$ has been interpreted as due to the vanishing of the helicity-flip amplitude at the zero in the ρ Regge trajectory by Arbab and Chiu [F. Arbab and C. B. Chiu, Phys. Rev. **147**, 1045 (1966)]. Their idea has been generalized to other reactions by Frautschi [S. Frautschi, Phys. Rev. Letters **17**, 722 (1966)].

²⁰ The expression for the expansion coefficients can be written in a relatively simple form. The calculation is tedious to perform by hand, however. We are grateful to Dr. Gerald Lynch for illuminating conversations on this point, and for the use of a computer program he has written to perform the expansion.

coefficients ($n \leq 5$), the expansion gives consistently larger values of A_n/A_0 than the fit to the differential cross section. For the high-order coefficients ($n \leq 6$), however, the agreement in size and energy dependence is remarkably good. This suggests, that the appearance of higher partial waves is dictated by the peripheral peak alone.

In the presence of an s -channel resonance strongly coupled to the ΔK^0 system, it may be expected that the coefficients A_n/A_0 will vary rapidly in the neighborhood of the resonance. The behavior of all coefficients shown on Fig. 6 is smooth; consequently the data show no evidence for any s -channel resonance. In particular we find no evidence for the process $\pi^- p \rightarrow N^*(2190) \rightarrow \Delta K^0$.

The $\Sigma^- K^+$ final state, in contrast to ΔK^0 and $\Sigma^0 K^0$ shows no peripheral peaking. What one observes is rather an "antiperipheral" peak, near $\cos\theta = -1$. This behavior follows the pattern of other reactions such as $K^- p \rightarrow \Xi^- K^+$, where the t -channel quantum numbers require the exchange of an $I = \frac{3}{2}$ strange meson. It is therefore plausible to assume that the dominant contribution to the reaction arises from *baryon exchange* in the u channel.²¹ Among the known baryons those with $I = 0$ or 1 can contribute in the $\Sigma^- K^+$ reaction. However, the lack of "antiperipheral" peaking in the $\Sigma^0 K^0$ case, where only $I = 1$ baryons could be exchanged, suggests the dominance of $I = 0$ exchange.²²

In analogy with Eq. (7) we define the Lorentz-invariant four-momentum transfer squared in the u

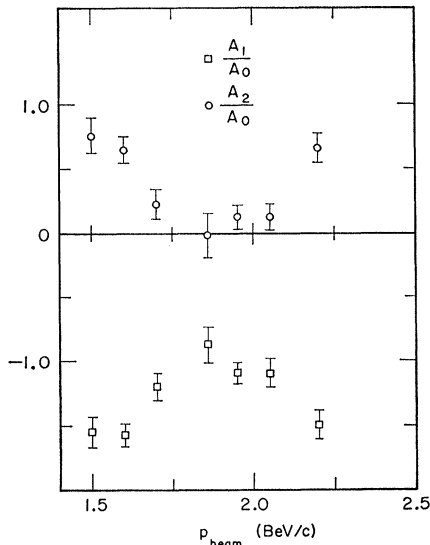


Fig. 8. Coefficients of the Legendre-polynomial fit to the $\pi^- p \rightarrow \Sigma^- K^+$ angular distribution as a function of the beam momentum.

²¹ For a review of the analysis of other reactions in terms of baryon exchange, see Peter E. Schlein, in *Lectures in Theoretical Physics* (University of Colorado, Boulder, Colorado, 1966), Vol. VIII B, p. 111; and L. Lyons, *Nuovo Cimento* 43, A888 (1966).

²² The contribution of $I = 1$ baryon exchange to $\Sigma^0 K^0$ would have to be twice as large as to $\Sigma^- K^+$.

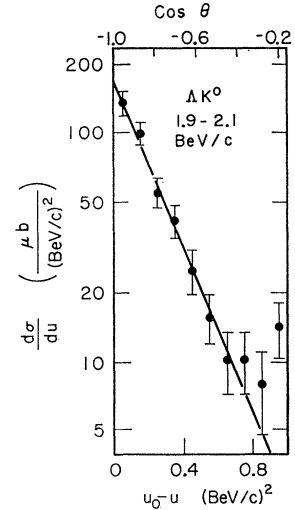


FIG. 9. Momentum-transfer distribution in the u channel for $\pi^- p \rightarrow \Delta K^0$ at 1.9- to 2.1-BeV/c beam momentum. The line represents a maximum-likelihood fit to the expression $d\sigma/du = C \exp[-D(u_0-u)]$ in the region $0 < u_0-u < 0.5$ (BeV/c)². The fit yields $D = 4.2 \pm 0.6$ (BeV/c)⁻².

channel as

$$u = (E_K - E_p)^2 - (\mathbf{p}_K - \mathbf{p}_p)^2. \quad (9)$$

In the c.m. system we have $du = -2p_K p_p d(\cos\theta)$. The maximum value u_0 occurs when $\cos\theta = -1$. The distribution in $u_0 - u$ is presented on Fig. 7. The line superimposed on the data represents a maximum-likelihood fit to the expression

$$\frac{d\sigma}{du} = C \exp[-D(u_0-u)] \quad (10)$$

in the region $0 \leq u_0 - u < 1$ (BeV/c)².

The $\Sigma^- K^+$ channel also differs from ΔK^0 and $\Sigma^0 K^0$ in the simplicity of its production angular distribution. The Legendre-polynomial fit is in reasonable agreement with the expansion of expression (10), [with $D = 1.4$ (BeV/c)⁻²] above 2.2 BeV/c. This behavior suggests that the interaction volume is considerably smaller for $\pi^- p \rightarrow \Sigma^- K^+$ than for $\pi^- p \rightarrow \Delta K^0, \Sigma^0 K^0$, or most other reactions. Below 2.2 BeV/c the fit to Legendre polynomials up to second order is adequate. To remove the dependence on the total cross section, we divide by A_0 ,

TABLE IV. Least-squares fit of the energy dependence of the cross sections to the expression $d\sigma/dt$ (or $d\sigma/du$) = $F E_{c.m.}^m$.

Reaction	Momentum-transfer interval (BeV/c) ²	Data points	χ^2	m
$\pi^- p \rightarrow \Delta K^0$	$0 < t_0 - t < 0.4$	10 ^a	15.8	-2.0 ± 0.4
	$0.4 < t_0 - t < 0.8$	10 ^a	8.5	-4.7 ± 0.5
	$0 < u_0 - u < 1.0$	10 ^a	18.3	-10.5 ± 0.6
$\pi^- p \rightarrow \Sigma^0 K^0$	$0 < t_0 - t < 0.4$	11	3.0	-1.5 ± 0.6
	$0.4 < t_0 - t < 0.8$	11	10.1	-5.1 ± 0.8
$\pi^- p \rightarrow \Sigma^- K^+$	$0 < u_0 - u < 1.0$	11	13.3	-9.8 ± 0.4
	$1.0 < u_0 - u < 2.0$	7 ^b	3.8	-11.5 ± 0.9

^a The point at 1.5 BeV/c was eliminated because it fell several standard deviations outside the fit.

^b Only data above 1.9 BeV/c were used, because at lower momentum, kinematics does not allow the momentum transfer $u_0 - u = 2$ (BeV/c)².

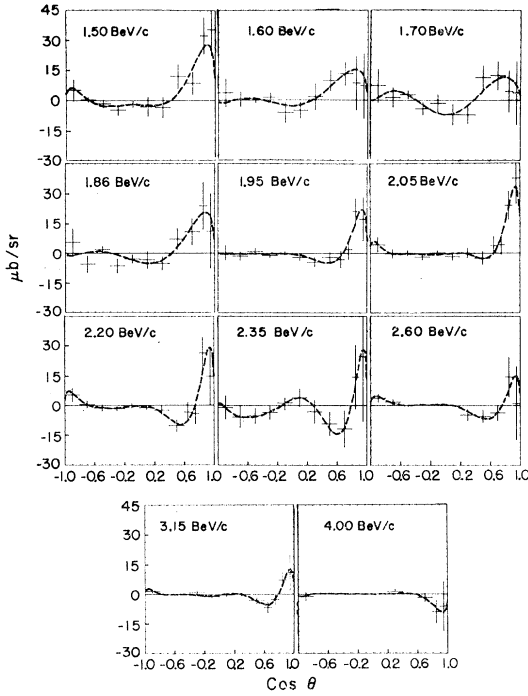


FIG. 10. Distribution of the quantity $\alpha_A \mathcal{P}(d\sigma/d\Omega)$ for the reaction $\pi^-p \rightarrow \Lambda K^0$. The angle θ is defined by $\cos\theta = \hat{p}_{K^0} \cdot \hat{p}_{\text{beam}}$ in the production c.m. system. The curves represent least-squares fits to the series $\sin\theta \sum_n B_n [dP_{n1+}(\cos\theta)]/d(\cos\theta)$. The data are also given in Table V, and the parameters of the fit in Table VI.

and present the ratios A_1/A_0 and A_2/A_0 on Fig. 8. It is interesting to note that the fitted coefficients A_1 and A_2 go through marked variations near 1.9 BeV/c. We have no explanation for the observed behavior.

The "antiperipheral" peak in the ΛK^0 final state can also be considered in terms of a baryon-exchange model. Here, as in the $\Sigma^0 K^0$ case, only hyperons with $I=1$ can contribute in the u channel.²³ In Fig. 9 we present the $d\sigma/du$ distribution in the 2-BeV/c region only. At higher energies the number of events near

²³ The relative size of the baryon exchange peaks in the three reactions considered can be understood in the framework of SU_3 invariance. If we assume that the $I=0$ contribution comes from Λ , and that the $I=1$ contribution comes from Σ and $Y_1^*(1385)$ exchange, the amplitudes for the three reactions become

$$\begin{aligned} A_{\Sigma^- K^+} &= C_1 \Sigma + C_2 Y_1^*(1385) + C_3 \Lambda, \\ A_{\Sigma^0 K^0} &= -\sqrt{2} C_1 \Sigma - \sqrt{2} C_2 Y_1^*(1385), \\ A_{\Lambda K^0} &= C_4 \Sigma - (\sqrt{6}) C_2 Y_1^*(1385), \end{aligned}$$

where the particle symbols on the right represent the contribution from the exchange of that object. If the ratio of d - and f -type coupling is $d/f > 1.0$, we find that (a) $C_3/C_1 \geq 3$, and (b) the relative sign of the coefficients for Σ and $Y_1^*(1385)$ is different for $\pi^-p \rightarrow \Lambda K^0$ and for $\pi^-p \rightarrow \Sigma K$. For $d/f = 1.5$, for example, we have $C_1 = 4/25$, $C_2 = 1/6$, $C_3 = 18/25$, and $C_4 = (2\sqrt{6})/25$. The lack of a baryon exchange peak in the $\pi^-p \rightarrow \Sigma^0 K^0$ differential cross section can then be interpreted as destructive interference between the Σ and the $Y_1^*(1385)$. The same holds for $\pi^-p \rightarrow \Sigma^- K^+$, and Λ exchange is expected to give a large cross section. For the reaction $\pi^-p \rightarrow \Lambda K^0$ the interference between Σ and $Y_1^*(1385)$ becomes constructive, and a sizeable baryon exchange peak can be expected, as is found in the experiment. We thank Professor David Jackson for bringing this argument to our attention.

TABLE V. Distribution of the polarization times the differential cross section for the reaction $\pi^-p \rightarrow \Lambda K^0$. The values of $\alpha \mathcal{P}(d\sigma/d\Omega)$ are given in units of $\mu\text{b}/\text{sr}$ as a function of beam momentum and production angle.

\hat{p}_{beam} (BeV/c)	$\cos\theta = -1.0$	-0.8	-0.6	-0.4	-0.2	0.0	0.2	0.4	0.6	0.8	0.9	1.0
1.50	10.0±10.4	0.7±1.9	0.7±1.9	-3.1±3.5	-9.4±4.9	-3.6±2.7	-6.2±9.2	-7.0±10.2	23.6±11.7	16.9±10.8	64.2±18.2	70.4±25.6
1.60	3.6±6.9	0.4±3.5	-0.1±1.2	-0.1±1.2	1.3±2.1	-6.1±5.1	-5.1±3.9	1.6±6.2	9.5±4.9	12.9±5.7	8.4±13.1	7.0±16.0
1.70	7.0±8.2	1.3±4.7	2.7±1.9	2.7±1.9	-4.1±2.9	-1.5±4.2	-7.1±5.0	-7.2±4.2	11.1±5.7	12.0±7.0	4.3±10.1	3.5±15.6
1.86	5.3±6.9	-5.7±4.1	1.8±1.6	1.8±1.6	-6.6±3.5	-3.0±2.1	-3.5±4.4	-5.3±3.3	7.1±5.3	10.9±6.6	23.8±11.7	11.1±18.8
1.95	0.2±3.6	-1.5±2.1	1.0±1.5	1.0±1.5	-1.2±0.9	0.0±0.7	-2.1±1.6	-4.4±2.3	-2.1±2.6	-0.6±3.2	21.2±6.4	17.3±10.8
2.05	4.4±3.7	-0.2±2.2	0.1±1.3	0.1±1.3	-1.9±1.4	0.3±1.1	-1.9±1.8	0.2±2.3	-2.6±3.3	4.0±3.4	24.0±7.0	37.5±12.5
2.20	5.3±3.4	0.5±1.7	-1.3±1.5	-1.3±1.5	-1.7±1.1	-0.2±1.1	-1.2±0.9	-2.5±1.9	-10.4±2.9	-3.8±3.5	26.3±7.8	14.7±14.3
2.35	-1.2±5.7	-5.9±5.3	-5.3±3.8	-5.3±3.8	-3.5±3.5	1.2±3.6	3.9±4.4	-3.2±5.8	-9.3±5.9	-11.9±9.1	14.2±16.0	24.4±32.4
2.60	3.6±2.0	1.7±1.3	-0.0±0.4	-0.0±0.4	0.4±0.4	0.5±0.5	-0.0±0.4	-4.8±2.7	-5.4±3.0	-3.7±3.8	14.3±9.9	1.0±18.3
3.15	1.6±0.8	-0.0±0.1	-0.1±0.1	-0.1±0.1	1.0±0.8	-1.2±0.7	-0.3±0.7	0.0±0.7	-3.2±1.5	-4.8±1.7	7.2±3.6	10.8±8.7
4.00	-1.1±2.0	0.3±0.3	-0.0±0.2	-0.0±0.2	-0.0±0.2	-0.0±0.2	-0.0±0.2	1.2±1.2	-0.0±0.2	-1.9±2.0	-9.0±5.7	-6.3±12.3

TABLE VI. Coefficients of the least-squares fit of the angular distribution of Λ polarization in the reaction $\pi^-p \rightarrow \Lambda K^0$ to the series $\alpha \mathcal{P} d\sigma/d\Omega = \sin\theta \sum_n B_n [dP_{n+1}(\cos\theta)/d(\cos\theta)]$.

p_{beam} (BeV/c)	χ^2	Probability (%)	B_0	B_1	B_2	B_3	B_4	B_5	B_6
1.50	6.66	35.4	+5.0±2.8	+9.1±2.5	+10.8±2.2	+4.2±2.0	+3.6±1.7		
1.60	3.72	71.5	+2.4±1.7	+3.7±1.5	+3.1±1.5	+1.2±1.2	-0.3±1.1		
1.70	5.78	44.8	+5.0±1.8	+1.7±1.6	+3.9±1.6	+0.8±1.2	-0.9±1.1		
1.86	7.45	28.1	+1.1±1.6	+3.6±1.6	+4.2±1.5	+2.5±1.2	+0.2±1.0		
1.95	5.49	35.9	-0.2±0.8	+1.3±0.9	+2.3±0.8	+2.6±0.8	+1.9±0.7	+0.9±0.5	+0.3±0.5
2.05	4.74	44.8	+1.6±0.9	+2.3±0.9	+3.7±0.9	+2.6±0.8	+3.0±0.8	+1.3±0.6	+0.9±0.5
2.20	5.53	35.5	-1.1±0.8	-0.1±0.9	+2.8±0.9	+2.3±0.9	+3.4±0.8	+1.4±0.6	+0.8±0.5
2.35	0.35	98.6	-2.8±2.1	+0.8±2.2	-0.2±2.0	+2.1±1.9	+3.9±1.8	+2.1±1.5	+0.8±1.3
2.60	1.91	75.3	-0.4±0.8	-0.9±1.0	+1.4±1.0	+1.3±1.0	+2.0±0.9	+0.7±0.5	+0.3±0.4
3.15	6.19	28.8	-0.5±0.4	-0.3±0.4	+0.7±0.4	+0.7±0.4	+1.4±0.4	+0.9±0.3	+0.6±0.2
4.00	1.25	87.0	-0.7±0.4	-1.0±0.5	-1.1±0.6	-0.9±0.5	-0.7±0.4	-0.3±0.2	-0.2±0.2

$\cos\theta = -1$ is too small to give a meaningful spectrum.

We fitted the energy dependence of the differential cross section at constant momentum transfer to the expression

$$\frac{d\sigma}{dt} = FE_{e.m.}^m \quad (11)$$

in the region of the peripheral peaks. For the anti-peripheral peaks we fitted $d\sigma/du$ to an expression of the same form. Results of the fit are presented in Table IV. We note that

- (a) the values of the exponent m found for the ΛK^0 and $\Sigma^0 K^0$ data are similar for the peripheral peak;
- (b) the values of m found for the ΛK^0 and $\Sigma^- K^+$ data are similar for the antiperipheral peak;
- (c) the cross sections fall faster at larger momentum transfer. This "shrinking" of the peaks may indicate some Regge-type behavior.

The data presented allow us to make a few comments concerning the reaction $\pi^+p \rightarrow \Sigma^+ K^+$ in the 3- to 4-BeV/c range. We use the relation between the complex amplitudes A^+ , A^0 , and A^- for the reactions $\pi^+p \rightarrow \Sigma^+ K^+$, $\pi^-p \rightarrow \Sigma^0 K^0$, and $\pi^-p \rightarrow \Sigma^- K^+$, respectively. Charge independence predicts

$$A^- + \sqrt{2}A^0 = A^+. \quad (12)$$

Near $\cos\theta = +1$ the cross section for the $\Sigma^- K^+$ reaction is much smaller than that for $\Sigma^0 K^0$, and therefore A^- is small compared to A^0 (A^0 is small compared to A^- near $\cos\theta = -1$). In a first approximation we neglect the small amplitude, to obtain $(d\sigma/d\Omega)_{\Sigma^+ K^+} \approx 2(d\sigma/d\Omega)_{\Sigma^0 K^0}$ near $\cos\theta = +1$, and since the total cross section is dominated by the peripheral peak, we have $(\sigma_T)_{\Sigma^+ K^+} \sim 2(\sigma_T)_{\Sigma^0 K^0}$ above 3 BeV/c. In the same way we find that $(d\sigma/d\Omega)_{\Sigma^+ K^+}$ will have a small peak of the same order of magnitude as $(d\sigma/d\Omega)_{\Sigma^- K^+}$ near $\cos\theta = -1$.²⁴

²⁴ Data on the reaction $\pi^+p \rightarrow \Sigma^+ K^+$, and a comparison with the other ΣK channels along the lines outlined here have recently been presented. See R. R. Kofler, R. H. Hartung, and D. D. Reeder, contribution to the *XIIIth International Conference on High-Energy Physics, 1966, Berkeley, California* (University of California Press, Berkeley, 1967).

IV. POLARIZATION

For the reaction $\pi^-p \rightarrow \Lambda K^0$ the $\Lambda \rightarrow p\pi^-$ decay is a good analyzer of the Λ polarization. The angular distribution of the decay proton with respect to the production normal $\mathbf{n} = \mathbf{p}_{\text{beam}} \times \mathbf{p}_{K^0}$ is of the form $(1 + \alpha_\Lambda \mathcal{P} \cos\xi)$, where $\alpha_\Lambda = 0.66$ is the asymmetry parameter, \mathcal{P} is the polarization, and ξ is the angle between the momentum of the decay proton and \mathbf{n} in the Λ rest frame. The product of the differential cross section and the polarization at the production angle θ is given by

$$\alpha_\Lambda \mathcal{P}(\theta) \frac{d\sigma}{d\Omega} = 3c \sum_i \cos\xi_i,$$

where the sum is over the events within an interval of the production angle,²⁵ and the constant c converts this sum into cross-section units.

The results are presented in Fig. 10 and Table V. The curves on Fig. 10 represent least-squares fits to the form¹⁸

$$\alpha_\Lambda \mathcal{P}(\theta) \frac{d\sigma}{d\Omega} = \sin\theta \sum_n B_n \frac{dP_{n+1}(\cos\theta)}{d(\cos\theta)},$$

where P_n is the n th-order Legendre polynomial. The fitted coefficients B_n are shown in Table VI. In Fig. 11 we present the polarization as a function of the momentum transfer. The size and shape of the distribution are similar for the data near 2 and 3 BeV/c.²⁶ We find the polarization positive at low momentum transfer, then negative in the region $t - t_0 \approx -1$ (BeV/c)². The crossover point is near $t - t_0 = -0.5$ (BeV/c)². The

²⁵ Actually the term in the sums were weighted by the inverse of the detection probability ϵ_i . The complete sum, including the error is then

$$\sum_i \frac{\cos\xi_i}{\epsilon_i} \pm \left[\sum_i \left(\frac{\cos\xi_i}{\epsilon_i} \right)^2 \right]^{1/2}.$$

See F. T. Solmitz, *Ann. Rev. Nucl. Sci.* **14**, 375 (1964), especially p. 399.

²⁶ Our results are in good agreement with the polarization measurements at 1.5 BeV/c by Yoder *et al.* (Ref. 2), at 1.59 BeV/c by Goussu *et al.* (Ref. 3), and at 1.5 and 1.8 BeV/c by Kim *et al.* (Ref. 1).

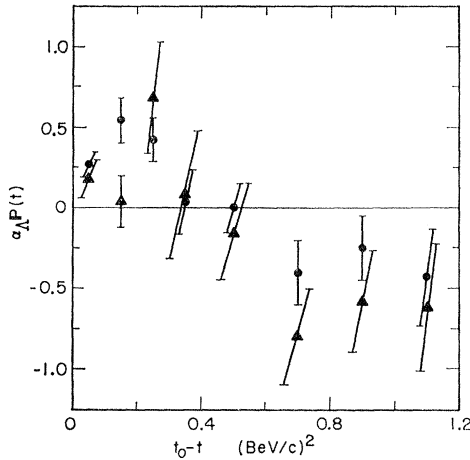


FIG. 11. Polarization of the Λ in the reaction $\pi^-p \rightarrow \Lambda K^0$ as a function of the momentum transfer squared. The data for the 1.9- to 2.1-BeV/c interval are shown as circles; those for the 2.9- to 3.3-BeV/c interval are shown as triangles.

largest negative value of the polarization remains consistent with 100% even at the highest beam momenta.

We note that the simplest one-particle- and one-Regge-pole-exchange models predict no polarization for the final-state hyperon. Using a model based on the exchange of both the $K^*(890)$ and $K^*(1410)$ Regge trajectories, Sarma and Reeder²⁷ successfully fitted both the angular distribution and the Σ^+ polarization in the reaction $\pi^+p \rightarrow \Sigma^+K^+$ at 3.23 BeV/c.²⁴ Since the qualitative features of the Σ^+K^+ channel are strikingly similar to the data presented here, extension of their analysis to include the ΛK^0 final state seems highly desirable.²⁸

Due to lack of statistics in Σ^0 and to the small value of the asymmetry parameter in Σ^- decay, we have no significant results on Σ polarization.²⁹

²⁷ K. V. L. Sarma and D. D. Reeder, University of Wisconsin Report, 1966 (unpublished).

²⁸ A model involving two Regge-pole exchange has also been developed by Arnold [R. C. Arnold, Phys. Rev. **153**, 1506 (1967)].

²⁹ Polarization of the Σ^0 has been measured at 1.5 and 1.8 BeV/c by Y. S. Kim, G. R. Burleson, P. I. P. Kalmus, A. Roberts, and T. A. Romanowsky, Phys. Rev. **143**, 1028 (1966).

V. SUMMARY

In summary, we find that the dominant features of the reactions $\pi^-p \rightarrow \Lambda K^0$, $\Sigma^0 K^0$, and $\Sigma^- K^+$ can be described in terms of meson and baryon exchange in the t and u channels, respectively. All cross sections decrease with increasing beam momentum, more slowly for meson exchange than for baryon exchange. The polarization of the Λ in $\pi^-p \rightarrow \Lambda K^0$ remains large in the region of moderate momentum transfer [$|t| \leq 1(\text{BeV}/c)^2$], even at the highest energies available in this experiment.

The energy dependence of the total cross sections and the momentum-transfer distribution is suggestive of Regge-type behavior. In terms of the Regge picture the observed polarization requires that two K^* trajectories contribute to $\pi^-p \rightarrow \Lambda K^0$.

The results presented indicate a break in the peripheral peaks near $t-t_0 = -0.5(\text{BeV}/c)^2$ and a change of sign of the Λ polarization at about the same value of the momentum transfer. Similar phenomena observed in several other reactions^{24,30} have been associated with the passage of the exchanged Regge trajectories through zero.^{19,27}

ACKNOWLEDGMENTS

We wish to thank the scanning and measuring staff for their untiring efforts, and members of the Bevatron and bubble-chamber operations groups for the excellent cooperation we received at the time of the exposure. Dr. Gideon Alexander, Dr. George R. Kalbfleisch, and Dr. Gerald A. Smith have participated in the analysis of the first stages of the experiment. We are grateful to Professor David Jackson for helpful comments. It is a pleasure to thank Professor Luis W. Alvarez for his encouragement and support, and members of the Alvarez Group for their help and criticism.

³⁰ For a list of references on this subject see S. Frautschi, Ref. 19.